

Tomography of the Earth's Core Using Supernova Neutrinos

Manfred Lindner^a, Tommy Ohlsson^{ab,y}, Ricard Tomas^{cz}, Walter Winter^{ax}^aInstitut für Theoretische Physik, Physik-Department, Technische Universität München,
James-Frank-Straße, 85748 Garching bei München, Germany^bDivision of Mathematical Physics, Department of Physics, Royal Institute of Technology (KTH) –
Stockholm Center for Physics, Astronomy, and Biotechnology, 106 91 Stockholm, Sweden^cMax-Planck-Institut für Physik (Werner-Heisenberg-Institut), Fohringer Ring 6, 80805 München,
Germany

Abstract

We investigate the possibility to use the neutrinos coming from a future galactic supernova explosion to perform neutrino oscillation tomography of the Earth's core. We propose to be using existing or planned detectors, resulting in an additional payoff. Provided that all of the discussed uncertainties can be reduced as expected, we find that the average densities of the Earth's inner and outer cores could be measured with a precision competitive with geophysics. However, since seismic waves are more sensitive to matter density jumps than average matter densities, neutrino physics would give partly complementary information.

PACS: 14.60.Lm; 13.15.+g; 91.35.-x; 97.60.Bw

Key words: Neutrino oscillations; Supernova neutrinos; Neutrino tomography; Geophysics

1. Introduction

In order to obtain more information about the interior of the Earth, neutrino tomography has been considered as an alternative method to geophysics. There exist, in principle, two different such techniques, neutrino absorption tomography [1{9] and neutrino oscillation tomography [10{14]. Neutrino absorption tomography, based on the absorption of neutrinos in matter, is in some sense similar to X-ray tomography and unfortunately faces several problems including the need of extremely high energetic neutrino sources, huge detectors, and the prerequisite of many baselines. Neutrino oscillation tomography uses the fact that neutrino oscillations are influenced by the presence of matter [15{17]. Neutrino oscillation tomography would, in principle, be possible with a single baseline, since interference effects provide additional information on the matter density profile. However, it requires

quite precise knowledge about the neutrino oscillation parameters and stringent bounds on the contribution of non-oscillation physics, such as neutrino decay, CPT violation, non-standard interactions, sterile neutrinos, etc. Supernovae as neutrino sources are especially interesting, since the neutrinos come in large numbers from a short burst, which could be used to obtain a snapshot of the Earth's interior. In addition, compared to solar neutrinos, their energy spectrum has a high-energy tail, which is more sensitive to Earth matter effects. The influence of Earth matter on supernova neutrinos has, for example, been studied in Refs. [18{20].

We assume that technologically feasible detectors exist, such as Super-Kamiokande, SNO, Hyper-Kamiokande, and UNO, which are originally built for different purposes, but also capable to detect supernova neutrinos. We discuss the possibility to use the neutrinos coming from a future galactic supernova explosion to determine with the assumed detectors some of the measurable quantities describing the structure of the Earth's interior. We especially focus on the outer and inner core of the Earth, since they are

E-mail: lindner@ph.tum.de

yE-mail: tohlsson@ph.tum.de, tommy@theophys.kth.se

zE-mail: ricard@mppmu.mpg.de

xE-mail: wwinter@ph.tum.de

much harder to access with conventional geophysical methods than the mantle of the Earth.

2. Geophysical aspects

In geophysics, the most promising technique to access the Earth's interior is to use seismic wave propagation (for a summary, see Refs. [21,22]). Especially, the detection of seismic waves produced by earthquakes gives valuable information on the seismic wave velocity profile of the Earth matter. However, the matter density is not directly accessible, but indirectly obtained by assumptions about the equation of state of the considered materials. Since seismic S-waves are mainly reflected at the mantle-core boundary, information on the Earth's core is much harder to obtain than on the Earth's mantle. Therefore, we will especially focus on the Earth's core in this paper. Since reflection and refraction of P-waves at transition boundaries with large matter density contrasts are quite easy to observe with seismic waves, the mantle-core and outer core-inner core boundaries can be located with high precision as well as the matter density jumps can be measured. For example, the matter density jump at the outer core-inner core boundary is often given by $(0.55 \pm 0.05) \text{ g/cm}^3$ [23]. This is quite a difference compared to neutrino physics, since neutrino oscillations in matter are especially sensitive to the average matter densities (on the scale of the neutrino oscillation length) indirectly measured by the electron density. Thus, neutrino oscillations are less sensitive to local differences, but they involve less unknowns from the equation of state and could therefore access the absolute matter densities instead of the matter density jumps.

Several issues regarding the Earth's inner core are considered to be interesting from a geophysical point of view. For different indirect reasons the inner core is believed to consist mainly of iron and it is therefore often called the iron core. First of all, the spectral lines in the sunlight indicate that the atmosphere of the Sun partly consists of iron as a potential material source for the planets. A second hint comes from the magnetic field of the Earth. After all, there are no convincing alternatives. We will see later that neutrino tomography could directly verify the average matter density of an iron core. Further topics relevant for the inner core structure are: anisotropy, heterogeneity, time-dependence, solidity, and rotation (for a summary, see Ref. [24]). However, since neutrino oscillations are to a good approximation only sensitive to average matter densities at long scales, these issues are much harder to access with neutrino oscillation tomography.

3. Core-collapse supernovae as neutrino sources

Core-collapse supernovae represent the evolutionary end of massive stars with a mass $M < 8M_{\odot}$, where M_{\odot} is the mass of the Sun. In these explosions, about 99% of the liberated gravitational binding energy, $E_b \approx 3 \cdot 10^{51} \text{ erg}$, is carried away by neutrinos in roughly equal amounts of energy for all flavors in the first 10 seconds after the onset of the core collapse [25]. It is widely believed that the time-dependent energy spectrum of each neutrino species can be approximated by a "pinched" Fermi-Dirac distribution [26,28]. In this work, we assume that the time-integrated spectra can also be well approximated by the pinched Fermi-Dirac distributions with an effective degeneracy parameter μ , i.e.,

$$N^0(E) = \frac{E^{\text{tot}}}{hE} \frac{1}{iF_2(\mu)} \frac{E^2}{e^{E/T} + 1}; \quad (1)$$

where $E^{\text{tot}} = \int_0^R L dt$ is the total neutrino energy of a certain flavor ν ,

$$F_k(\mu) = \int_0^{\infty} \frac{x^k}{e^{x+\mu} + 1} dx;$$

and E and T denote the neutrino energy and the effective temperature, respectively. The relation between the average neutrino energy and the effective neutrino temperature is given by

$$hE_{\nu} = \frac{\int_0^{\infty} E N^0 dE}{\int_0^{\infty} N^0 dE} = \frac{F_3(\mu)}{F_2(\mu)} T; \quad (2)$$

For simplicity we assume that $\mu = 0$ for all neutrino flavors, which means that

$$hE_{\nu} = \frac{F_3(0)}{F_2(0)} T = \frac{7}{180} T \approx 0.039 \text{ kT}; \quad (3)$$

where $\zeta(x)$ is the Riemann z-function [31, 2026] and $k' = 3.15137$. Furthermore, the time-integrated flux of the neutrinos can be expressed by

$$\Phi_0 = \frac{N^0}{4 D^2}; \quad (4)$$

where D is the distance to the supernova.

Due to the different trapping processes, the different neutrino flavors originate in layers of the supernova with different temperatures. The electron (anti)neutrino flavor is kept in thermal equilibrium by processes up to a certain radius usually referred to as the "neutrinosphere", beyond which the neutrinos stream off freely. However, the practical absence of muons and taus in the supernova core implies that the other two neutrino flavors, here collectively denoted by ν_x ($\nu_\mu; \nu_\tau$), interact primarily by less efficient neutral-current processes. Therefore, their spectra are determined at deeper, i.e., hotter regions. In addition, since the content of neutrons is larger than that of protons, $\bar{\nu}_e$'s escape from outer regions than ν_e 's. This rough picture leads to the following hierarchy: $\langle E_{\bar{\nu}_e} \rangle < \langle E_{\nu_e} \rangle < \langle E_{\nu_x} \rangle$. Here ν_x refers again to both ν_μ and ν_τ . Typical values of the average energies of the time-integrated neutrino spectra obtained in simulations are $\langle E_{\bar{\nu}_e} \rangle = 12$ MeV, $\langle E_{\nu_e} \rangle = 15$ MeV, and $\langle E_{\nu_x} \rangle = 24$ MeV [29,30]. However, recent studies with an improved treatment of neutrino transport, microphysics, the inclusion of the nucleon bremsstrahlung, and the energy transfer by recoils, find somewhat smaller differences between the $\bar{\nu}_e$ and ν_x spectra [31,32].

In the following, we assume a future galactic supernova explosion at a typical distance of $D = 10$ kpc, with a binding energy of $E_b = 3 \times 10^{51}$ erg and a total energy of $E_e^{\text{tot}} = E_{\bar{\nu}_e}^{\text{tot}} + E_{\nu_e}^{\text{tot}} + E_{\nu_x}^{\text{tot}}$, where α parameterizes a possible deviation from energy equipartition [33]. We also assume that the fluxes of $\bar{\nu}_e$, ν_e , ν_μ , and ν_τ are identical and we fix $\langle E_{\nu_e} \rangle$ to 15 MeV. We consider four scenarios with different values of the parameters α and β : $(\alpha, \beta) = (1, 2); (1, 4); (0.5, 1); (0.5, 1)$, as shown in Tab. 1.

As far as the neutrino detection is concerned, we only analyze the charged-current reaction $\bar{\nu}_e +$

Parameter	S1	S2	S3	S4
	1	1	0.5	0.5
β	1.4	1.2	1.4	1.2

Table 1

Our four different standard scenarios for supernova parameters, where in all cases $\langle E_{\bar{\nu}_e} \rangle = 15$ MeV.

$p \rightarrow e^+ + n$, since this reaction yields the largest number of events (around 8000 in the Super-Kamiokande detector in the case of a galactic supernova). Therefore, we shall concentrate on the study of the propagation of antineutrinos from a supernova to detectors on the Earth.

4. From neutrino production to neutrino detection

In general, neutrino propagation from a source to a detector is described by an evolution operator on the form

$$U = U(L) = e^{i \int_0^L H(L^0) dL^0}; \quad (5)$$

where $H = H(L)$ is the total Hamiltonian and L is the neutrino (traveling) path length, i.e., the baseline length. The Hamiltonian is usually given either in the flavor basis or in the mass basis. In the flavor basis, the total Hamiltonian reads $H_f(L) = U H_m U^\dagger + A(L) \text{diag}(1; 0; 0)$, where $H_m = \text{diag}(E_1; E_2; E_3)$ is the free Hamiltonian in the mass basis, $U = (U_{\alpha a})$ is the leptonic mixing matrix, and

$$A = A(L) = \frac{P}{2G_F} \frac{Y_e}{m_N} (L) \quad (6)$$

is the mass density parameter related to the matter density $\rho(L)$. Here $E_a = m_a^2 = (2E)$ ($a = 1; 2; 3$), $G_F = 1.16639 \times 10^{-5} \text{ eV}^{-2}$ is the Fermi weak coupling constant, Y_e is the average number of electrons per nucleon¹, and $m_N = 939 \text{ MeV}$ is the nucleon mass. The sign depends on the presence of neutrinos (+) or antineutrinos (-). Furthermore, m_a is the mass of the a th mass eigenstate and E is the neutrino energy. In

¹In the Earth: $Y_e = \frac{1}{2}$.

order to obtain the neutrino oscillation transition probabilities, we need to calculate the matrix elements of the evolution operator in the flavor basis, take the absolute values of these, and then square them. The neutrino oscillation probability amplitude from a neutrino flavor α to a neutrino flavor β is defined as

$$P_{\alpha\beta} = | \langle \nu_\beta | U_f(L) | \nu_\alpha \rangle |^2; \quad \alpha, \beta = e, \mu, \tau; \quad (7)$$

where U_f is the total evolution operator in the flavor basis. Then, the neutrino oscillation transition probability for $\alpha \rightarrow \beta$ is given by

$$P_{\alpha\beta} = | \langle \nu_\beta | U_f(L) | \nu_\alpha \rangle |^2; \quad \alpha, \beta = e, \mu, \tau; \quad (8)$$

The initial neutrino fluxes arise from the central part of the supernova, where the matter density is of the order of about 10^{12} g/cm^3 . For such high matter densities one can infer from the expression of the Hamiltonian H_f that the matter mass eigenstates, ν_a^m ($a = 1; 2; 3$), coincide with the flavor states, $(\nu = e, \mu, \tau)$, up to a rotation between ν_a^m and ν_α . Thus, in the case of normal mass hierarchy, $m_1 < m_2 < m_3$, one has

$$\nu_1^m = \nu_e; \quad \nu_2^m = \nu_\mu; \quad \nu_3^m = \nu_\tau; \quad (9)$$

where ν_a^0 and ν_α^0 are the rotated states. Therefore, one can assume that the original fluxes of the matter mass eigenstates are²

$$\nu_1^0 = \nu_e; \quad \nu_2^0 = \nu_\mu; \quad \nu_3^0 = \nu_\tau; \quad (10)$$

Since we are assuming that ν_e and ν_μ have the same fluxes, the neutrino transitions are determined by the mixings of the ν_e only, i.e., by $U_{e\alpha}$ [35]. Moreover, under the assumption of normal mass hierarchy, antineutrinos do not undergo any resonant conversion, which means that the small mixing angle θ_{13} is suppressed in matter and the $\nu_e \rightarrow \nu_3$ transitions are negligible. One

²Any rotation between ν_a^m and ν_α does not affect the corresponding total mass eigenstate contents, because they have the same fluxes, as discussed in the last section. For an analysis taking into account possible differences in the fluxes, see Ref. [34]. In addition, an argument against neutrino oscillations between ν_e and ν_μ on their way to the Earth will be given at the end of this section.

consequence is that ν_3^m propagates adiabatically and leaves the supernova as ν_3 . The propagation of the other two states depends on the parameters of the solution to the solar neutrino problem and it may be adiabatic or non-adiabatic [36,37]. In particular, we will focus on the Mikheyev-Smirnov-Wolfenstein (MSW) [15,17] large mixing angle (LMA) solution, since it is by far the most favored one. For the parameters within such a region the neutrino evolution through the supernova (SN) envelope is adiabatic. Thus, ν_e will leave the supernova as ν_1 , ν_μ as ν_2 , and ν_τ as ν_3 . Finally, the measured fluxes of supernova neutrinos at a detector on the Earth are

$$\Phi_a^0 = \sum_{\alpha=e,\mu,\tau} P_{\alpha a} \Phi_\alpha^0; \quad \alpha = e, \mu, \tau; \quad (11)$$

where Φ_a^0 ($a = 1; 2; 3$) are the initial supernova neutrino fluxes.

For neutrino propagation from a supernova (SN core) to a detector at the Earth (see Fig. 1) we have the probability amplitudes

$$A_{\alpha\beta} = | \langle \nu_\beta | U_f^{\text{tot}}(L) | \nu_\alpha \rangle |^2 = | \langle \nu_\beta | U(L) U^{\text{vac}}(L_{\text{vac}}) U^{\text{SN}}(L_{\text{SN}}) | \nu_\alpha \rangle |^2; \quad (12)$$

where U^{SN} , U^{vac} , and U are the evolution operators in the supernova (from SN core to SN envelope), in vacuum, and in the Earth, respectively, and L_{SN} , L_{vac} , and L are the corresponding baseline lengths. Note that the operators U^{SN} , U^{vac} , and U in general do not commute. Using the completeness relation, one can write the probability amplitudes as

$$A_{\alpha\beta} = \sum_{a=1}^3 | \langle \nu_\beta | U(L) U^{\text{vac}}(L_{\text{vac}}) | \nu_a \rangle |^2 | \langle \nu_a | U^{\text{SN}}(L_{\text{SN}}) | \nu_\alpha \rangle |^2; \quad (13)$$

Since we have seen that for adiabatic transitions the supernova neutrinos leave the supernova (SN envelope) as neutrino mass eigenstates ν_a , i.e., $\langle \nu_a | U^{\text{SN}}(L_{\text{SN}}) | \nu_\alpha \rangle = \delta_{\alpha a}$, we can redefine the probability amplitudes

$$A_{\alpha\beta} = | \langle \nu_\beta | U(L_E) U^{\text{vac}}(L_{\text{vac}}) | \nu_\alpha \rangle |^2; \quad (14)$$

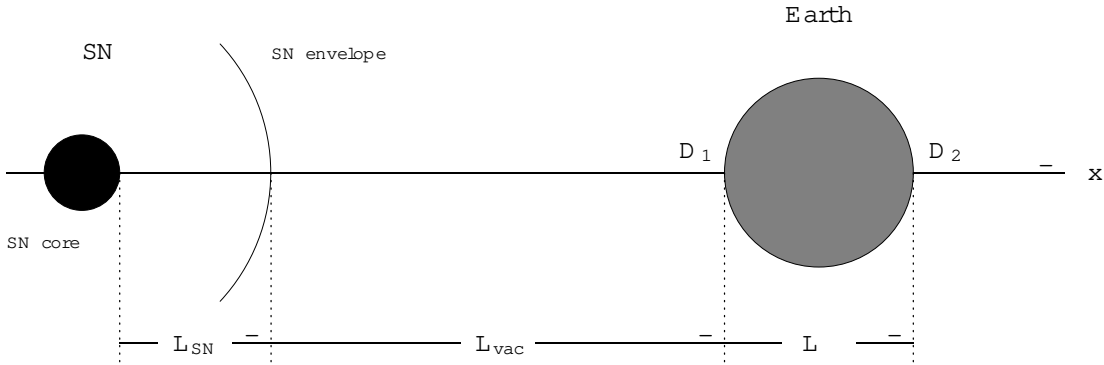


Figure 1. The propagation of neutrinos from a supernova (SN) to the Earth. The detector D_1 can be anywhere on the Earth's side towards the SN, whereas the detector D_2 should be in the shadow of the Earth's core.

where the first index is a mass eigenstate index ($a = 1; 2; 3$) and the second index is a flavor state index ($i = e; \mu; \tau$). These "mixed" probability amplitudes will completely determine the evolution of the neutrinos from a supernova (SN envelope) to the Earth. Now, there are, in principle, two cases for a supernova neutrino to be detected at the Earth (see again Fig. 1):

1. The supernova neutrino arrives at the detector from above, i.e., it does not go through the Earth at all (detector D_1).
2. The supernova neutrino goes through the Earth's core and then arrives at the detector (detector D_2).

Let us start with the first case. The probability amplitude for an initial neutrino mass eigenstate a , where $a = 1; 2; 3$, to leave the supernova and to oscillate into a flavor state i , where $i = e; \mu; \tau$, is at the detector D_1 given by

$$A_a^{D_1} = \langle j | U^{vac}(L_{vac}) | a \rangle \quad (15)$$

Note that we assumed that a neutrino mass eigenstate a left the supernova, and therefore, no evolution operator U^{SN} should appear in the above equation. Furthermore, since the supernova neutrino does not go through the Earth, there appears also no evolution operator U in this equa-

tion. Next, since the evolution operator in vacuum U^{vac} is diagonal in the mass basis, we find that Eq. (15) reduces to³

$$\begin{aligned} A_a^{D_1} &= \langle j | a \rangle = \sum_{b=1}^3 U_{bj} U_{ba} \\ &= \sum_{b=1}^3 U_{ba} U_{bj} = U_{aa} \end{aligned} \quad (16)$$

i.e., the probability amplitudes are just the matrix elements of the leptonic mixing matrix. Thus, we have $P_a^{D_1} = |A_a^{D_1}|^2 = |U_{aa}|^2$, and inserting this into Eq. (11), we obtain the supernova neutrino fluxes at the detector D_1 as

$$\Phi_a^{D_1} = \sum_{i=1}^3 |U_{ia}|^2 \Phi_a^0; \quad i = e; \mu; \tau \quad (17)$$

Assuming as in Eq. (10) that the initial fluxes of the second and third mass eigenstates are equal, i.e., $\Phi_2^0 = \Phi_3^0$, the electron antineutrino flux at the detector D_1 can be written as

$$\Phi_e^{D_1} = \Phi_1^0 |U_{e1}|^2 + f_R |U_{e2}|^2 + |U_{e3}|^2 \Phi_3^0 \quad (18)$$

³The neutrino flavor states are defined as follows: $|j\rangle = \sum_{a=1}^3 U_{ja} |a\rangle$ ($i = e; \mu; \tau$), which implies that $\langle j | i \rangle = \sum_{a=1}^3 U_{ja} U_{ia}$. Here the U_{ja} 's are the matrix elements of the leptonic mixing matrix U .

Here $f_R = \frac{P_{21}^{D_1} - P_{12}^{D_1}}{P_{11}^{D_1} - P_{22}^{D_1}}$ is the so-called flux ratio, which is plotted for several values of ξ and τ (introduced in the last section) in Fig. 2. Furthermore, the flux ratio f_R depends on the supernova parameters $\hbar E_e$, τ , and ξ only and reads for $\tau = 0$

$$f_R = \frac{e^{\frac{k\xi}{\hbar E_e} + 1}}{4 e^{\frac{k\xi}{\hbar E_e} + 1} + 1}; \quad (19)$$

where again $k = 3.15137$. Reinserting the proba-

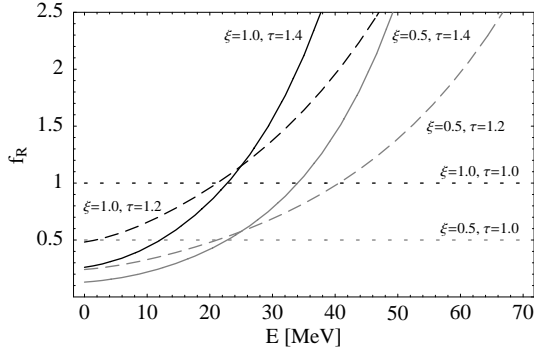


Figure 2. The flux ratio f_R as a function of the neutrino energy E for different values of the parameters ξ and τ , partly corresponding to the scenarios in Tab. 1.

bilities $P_{ae}^{D_1}$ instead of the probability amplitudes U_{ea} in Eq. (18) and using the unitarity condition $P_{1e}^{D_1} + P_{2e}^{D_1} + P_{3e}^{D_1} = 1$, we find that

$$P_{1e}^{D_1} = P_{1e}^{D_1} + f_R \frac{1 - P_{1e}^{D_1}}{P_{1e}^{D_1}}; \quad (20)$$

which means that the flux of electron antineutrinos at the detector D_1 is only depending on the initial neutrino flux \mathcal{J}_1^0 , the transition probability $P_{1e}^{D_1} = \mathcal{J}_{e1} \mathcal{J}_1^0$, and the flux ratio f_R .

Next, let us discuss the second case. Again using the fact that the evolution operator in vacuum

U^{vac} is diagonal in the mass basis, we find that

$$\begin{aligned} A_a^{D_2} &= \mathcal{J}_a \mathcal{J}_a^0 U^{\text{vac}}(L_{\text{vac}}) \mathcal{J}_a^0 \\ &= \sum_{b=1}^3 X^3 \mathcal{J}_a \mathcal{J}_a^0 \mathcal{J}_{b1} \mathcal{J}_b^0 U^{\text{vac}}(L_{\text{vac}}) \mathcal{J}_a^0 \\ &= \sum_{b=1}^3 X^3 \mathcal{J}_a \mathcal{J}_a^0 \mathcal{J}_{b1} \mathcal{J}_b^0 \\ &= \mathcal{J}_a \mathcal{J}_a^0 = A_a : \end{aligned} \quad (21)$$

Similar to the first case, we obtain the supernova neutrino fluxes at the detector D_2 as

$$D_2 = \sum_{a=1}^3 \mathcal{J}_a \mathcal{J}_a^0; \quad \mathcal{J}_a = e; \quad (22)$$

which for the electron antineutrino flux at the detector D_2 can be written as

$$D_2 = P_{1e}^{D_2} + f_R \frac{1 - P_{1e}^{D_2}}{P_{1e}^{D_2}}; \quad (23)$$

This means that the flux of electron antineutrinos at the detector D_2 depends only on the initial neutrino flux \mathcal{J}_1^0 , the transition probability $P_{1e}^{D_2} = \mathcal{J}_{1e} \mathcal{J}_1^0$, and the flux ratio f_R .

Now, we want to determine the neutrino oscillation transition probabilities. Using the evolution operator method developed in Ref. [38], the evolution operator in the Earth, which we will assume to consist of N different (constant) matter density layers, is given by

$$\begin{aligned} U(L) &= U(L_N; A_N) U(L_{N-1}; A_{N-1}) \dots \\ &= U(L_2; A_2) U(L_1; A_1) \\ &= \prod_{k=1}^N U(L_k; A_k); \end{aligned} \quad (24)$$

where $U(L_k; A_k) = e^{iH(A_k)L_k}$ is the evolution operator in the k th layer with constant matter density and $L = \sum_{k=1}^N L_k$.⁴ Here L_k and A_k are the thickness and matter density parameters of the k th matter density layer, respectively. Note

⁴ Similar applications of the evolution operator for propagation of neutrinos in matter consisting of two density layers using two neutrino flavors have been discussed in Refs. [39,40].

again that the evolution operators in the different layers normally do not commute. Inserting Eq. (24) into Eq. (21) and the result thereof into $P_a^{D_2} = \mathcal{A}_a^{D_2} \mathcal{J}$, we finally obtain

$$P_a^{D_2} = \sum_{k=1}^N U(L_k; A_k) \mathcal{J}_a^i ; \quad (25)$$

which is our main formula for the neutrino oscillation transition probabilities from a supernova to the detector D_2 . Thus, inserting $a = 1$ and $\mathcal{J} = e$ into Eq. (25), we find the probability $P_{1e}^{D_2}$, which can then be inserted into Eq. (23).

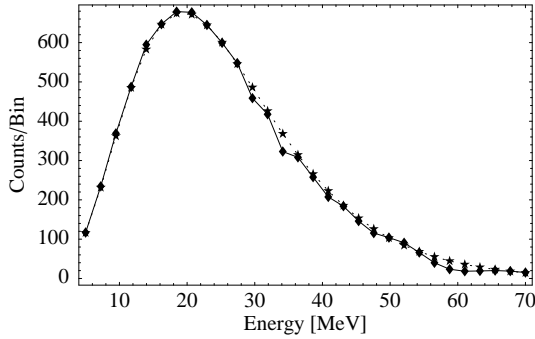


Figure 3. The charged-current events per energy bin from electron antineutrinos in an Super-Kamokande-like detector for a bin width of approximately 2.1 MeV , corresponding to an energy resolution of about 15% at 15 MeV . The solid curve shows the spectrum (scenario S1 in Tab. 1) including the Earth matter effects for a baseline of about 12700 km through the Earth's core, whereas the dashed curve shows the spectrum without Earth matter effects. The differences appear to be small, but are nevertheless statistically significant.

In Fig. 3, we show for the scenario S1 in Tab. 1 the different binned energy spectra at Super-Kamokande-like detectors, where the solid curve represents the detector D_2 and the dashed curve the detector D_1 . One can easily see that matter effects are largest for energies above about 25 MeV . For a detailed discussion of Earth matter

effects of supernova neutrinos, see Refs. [18, 20] and references therein. In summary, for our chosen values of the neutrino oscillation parameters (MSW-LMA solution, maximal atmospheric mixing, and normal mass hierarchy) the relative size of the Earth matter effects increases with energy and can be seen as oscillatory modulation of the energy spectrum. For small energies, however, this modulation oscillates too fast to be resolved, i.e., it averages out. For large energies about 25 MeV , the frequency becomes smaller and this modulation can be resolved. In Fig. 3, we used the scenario S1 from Tab. 1, making it possible that the fluxes of ν_x dominate above the critical energy around 25 MeV . This results in a negative modulation of the electron antineutrino spectrum, i.e., regeneration effects of ν_e and $\bar{\nu}_e$, as it is shown in Ref. [18]. However, a general suppression of the fluxes of the ν_x is possible for a value $\theta_{13} < 1$, which means that the modulation can be positive. From Fig. 3, it is also interesting to observe that solar neutrinos show much smaller Earth matter effects (day-night), since the spectrum is cut off far below 25 MeV . Thus, especially the high-energy tail in the supernova neutrino spectrum can make this application possible compared with solar neutrinos.

Let us now go back to Fig. 2, which shows the flux ratio f_R of the ν_x and the ν_1 fluxes at the surface of the Earth for the supernova parameter scenarios in Tab. 1. With Eq. (23) and this figure, we can estimate the sensitivity for different sets of supernova parameters. This equation describes the flux at the detector D_2 and depends on three different quantities. The flux Φ_1^0 can be indirectly determined by the detector D_1 , as it appears in Eq. (20) as the overall normalization. The flux ratio f_R depends on the supernova parameters θ_{13} and θ_{23} only, which can, up to a certain precision, also be reconstructed from the spectrum at the detector D_1 (cf., discussion in Sec. 7 and Ref. [41]). Note that it could be directly measured if one were also able to detect flavors other than the electron antineutrino, and the supernova parameters would completely drop out (cf., Eq. (17)). The transition probability $P_{1e}^{D_2}$ contains the information about the Earth matter and is usually quite large. Thus,

the ratio $(1 - P_{1e}^{D_2}) = P_{1e}^{D_2}$ in Eq. (23) is rather sensitive to changes in the Earth matter effects. Since this factor is multiplied with f_R , the energy-dependent flux ratio can enhance or suppress it. We have also noticed above that the (relative) Earth matter effects are increasing with energy. For the supernova parameters we can then distinguish three different cases, which can also be found in Fig. 2:

1. $\mu_e = 1, \mu_x = 1$ (energy equipartition and equal temperatures for all flavors): The flux ratio f_R is equal to unity (cf., Eq. (19)). Then, the neutrino transition probabilities in Eq. (23) drop out and we cannot use the supernova neutrinos for Earth matter effects.
2. $\mu_e = 1, \mu_x > 1$ (energy equipartition and a lower temperature for ν_e than for ν_x): The flux ratio f_R is enhanced for large energies, where Earth matter effects are large. The larger μ_x is, the larger becomes this effect. Thus, the scenario S2 in Tab. 1 performs worse than the scenario S1.
3. $\mu_e > 1, \mu_x = 1$ (more electron antineutrinos produced than the other two flavors): The flux ratio f_R / μ_e is suppressed in general. Therefore, the scenarios S3 and S4 are not as good for our application as the scenario S1.

Thus, the closeness to the equipartition of energies and the difference of the temperatures of the ν_e and ν_x are very important and we will therefore mainly focus now on the scenario S1.

For our application we assume that neutrino mass eigenstates arrive at the Earth and no neutrino oscillations take place between the supernova envelope and the surface of the Earth. This can either be justified by the adiabaticity condition for the propagation within the supernova, making mass eigenstates emerge from it, or by decoherence of neutrino oscillations between the surface of the supernova and the Earth. In both cases, Eq. (13) can be split into two independent factors without interference terms. The issue of wave packet decoherence has, for example, been

addressed in Refs. [42-47]. It has been found that neutrino oscillations vanish for neutrino propagation over distances much larger than the coherence length of the neutrino oscillations. This means that for $L > L_{ab}^{coh} / E^2 = m_{ab}^2$ the $L=E$ -dependent interference terms produced by the superposition of the mass eigenstates m_a and m_b in the neutrino oscillation formulas are averaged out. The quantity corresponds to a wave packet width determined by the production and detection processes [43,45]. Since for supernova neutrinos the distance of the propagation is especially large, it is plausible to assume that this averaging takes place and neutrino oscillations vanish by natural decoherence. In other words, the different group velocities of the wave packets of different mass eigenstates combine with dispersive effects such that the overlap of the mass eigenstates is gradually reduced to zero by a factor of $\exp[-(L_{ab}^{coh})^2]$ in the neutrino oscillation formulas. Hence, for $L > L_{ab}^{coh}$ the mass eigenstates arrive separately and the coherent transition amplitude in Eq. (12) is split up into two parts to be summed over incoherently (see, e.g., Ref. [46]), having the same effect as the adiabatic transition within the supernova separating the flavor states into mass eigenstates. Thus, it is reasonable to assume that mass eigenstates arrive at the surface of the Earth even for non-adiabatic transitions within the supernova.

Finally, in our numerical analysis, we assume Super-Kamiokande-like water-Cherenkov detectors, i.e., a 32 kt fiducial mass (for supernova neutrinos) Super-Kamiokande detector and a 1 Mt fiducial mass (for solar neutrinos) Hyper-Kamiokande detector. We choose 30 energy bins between the threshold energy 5 MeV and 70 MeV, since above 70 MeV the number of events is rather low. The bin width of approximately 2.1 MeV corresponds to an energy resolution of about 15% at 15 MeV.

5. A neutrino oscillation tomography model

We now introduce and discuss a simple model used for supernova neutrino tomography. As shown in Fig. 4, we assume at least two baselines

ending at detectors with similar statistics and systematics, such as Super-Kamiokande-like water-Cherenkov detectors. In order to measure the

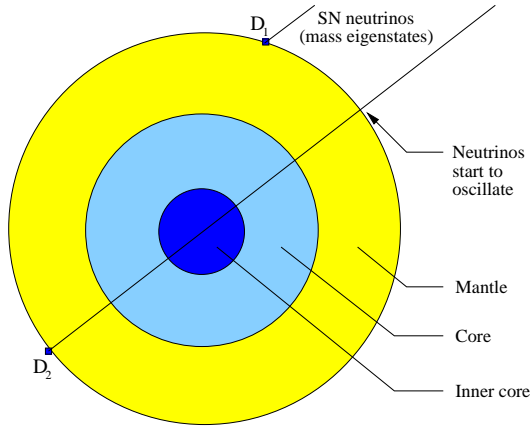


Figure 4. The minimal required setup for supernova neutrino tomography with at least two baselines, one of which is ending at the surface of the Earth at the detector D_1 , the other one is going through the Earth's core (or even the Earth's inner core) to the detector D_2 . In general, we assume that the neutrinos arrive as mass eigenstates at the detector D_1 and start to oscillate when they enter the Earth's interior.

reference spectrum of the supernova neutrinos, the neutrinos detected at the detector D_1 must not cross the Earth. The probability that the supernova neutrinos are observed directly, i.e., without crossing the Earth, is 50% for each detector. If we want to obtain information on the Earth's core, then the second detector D_2 needs to observe the supernova neutrinos with a baseline crossing the Earth's core with a sufficient length. In Tab. 2, the probabilities for a single detector D_2 to observe the supernova neutrinos coming from a random, but fixed, direction through the Earth's mantle, core, and inner core are summarized. Since the probability for a baseline to cross the inner core (about 1%) is rather small, one needs luck or time to be able to apply this technique. However, the probability for

Region	Minimum L [km]	Probability
Mantle	0	50 %
Core	10,670	~ 8 %
Inner core	12,510	~ 1 %

Table 2

The different inner Earth regions observed by a single detector detecting supernova neutrinos. They require the minimum baselines L through the Earth, which happens with the shown probabilities for a single detector.

a baseline to cross the core (about 8%) is already quite large, which means that for more than one detector one of them could really be at the right place.

Further on, we assume that the detector D_1 is at least as good as the detector D_2 , which means that the statistics is limited by D_2 , and D_1 measures the reference flux $\Phi_e^{D_1}$ with sufficient precision. For the neutrino oscillation parameters we choose $\theta_{12} = 32.9^\circ$, $\theta_{13} = 5^\circ$, $\theta_{23} = 45^\circ$, $m_{21}^2 = 5.0 \cdot 10^5 \text{ eV}^2$, $m_{32}^2 = 2.5 \cdot 10^5 \text{ eV}^2$, and $\delta_{CP} = 0$ [48[52], i.e., a normal mass hierarchy. Matter effects on supernova neutrinos in the Earth are discussed in detail in Ref. [18], where it is also demonstrated that Earth matter effects would be suppressed for solutions other than the MSW-LMA solution. For our application the dominant neutrino oscillation parameters are the solar neutrino oscillation parameters m_{21}^2 and θ_{12} , as well as the matter effects depend on $\sin^2 2\theta_{13}$. Later, we will estimate the precision with which we need to know these parameters and we will test the influence of the size of $\sin^2 2\theta_{13}$. Note that we assume mass eigenstates arriving at the surface of the Earth. Therefore, if D_1 and D_2 were identical detectors, a direct comparison of their energy spectra would verify the existence of Earth matter effects immediately. For detectors of different types the energy spectra would supply similar information in an indirect way.

For the modeling of the matter density profile we choose the Preliminary Reference Earth Model (PREM) profile [53,54], as it is shown in Fig. 5,

and approximate it by layers of constant average

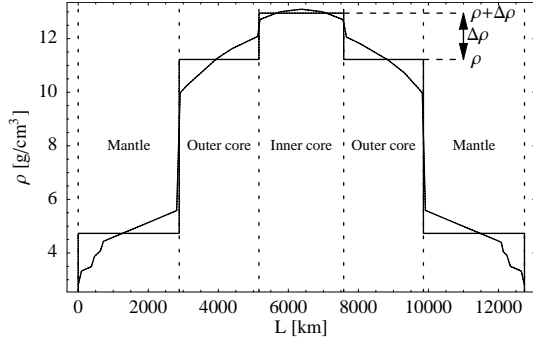


Figure 5. The model for the Earth’s matter density profile used in the calculations (step function) and the PREM matter density profile as function of the path length along the baseline shown in Fig. 4. The quantities which we are interested in are the average outer core matter density and the matter density jump between average inner and outer core densities, as it is shown in this figure.

matter densities. A baseline with a maximum length of twice the Earth radius then crosses the following layers in this order: mantle, outer core, inner core, outer core, mantle. Since substantial knowledge is provided by geophysics about the Earth’s mantle, we assume its matter density to be known with a sufficient precision. For such a baseline the interesting quantities to measure are the average outer core matter density and the matter density jump to the average inner core matter density, as illustrated in Fig. 5. This is slightly different to what is known from seismic wave geophysics, since there the density jumps of the actual matter densities at the mantle-core and outer-inner core boundaries are better known. However, since neutrino oscillations are not sensitive to matter densities at individual points, but essentially to the integral of the matter density and the length scale the neutrinos are traveling through [55], they are more appropriate to measure average matter densities.

The introduced model allows to estimate what could be learned from the neutrinos of a supernova explosion about the Earth’s interior. The actual situation, however, such as the number of detectors with baselines through the Earth, their size, the knowledge on the neutrino oscillation parameters, systematics, etc., can only be implemented after the next observed supernova explosion. Our discussion here serves only the purpose of demonstrating that such studies are feasible.

6. Results

Based on the modeling in the last section, we present results, which could be provided by a single supernova. Our analysis is performed with a standard χ^2 technique using [56]

$$\chi^2 = \sum_{i=1}^n \frac{(x_i - x_i^{\text{ref}})^2}{x_i^{\text{ref}}} ; \quad (26)$$

where n is the number of energy bins, x_i^{ref} is the reference event rate in the i th bin for the true parameters, and x_i is the measured/ varied event rate in the i th bin. The errors quoted are read off at the 2 confidence level (depending on the problem for one or two degrees of freedom). For two degrees of freedom we also take into account the two-parameter correlations. However, we assume that the effects of the systematics are negligible, i.e., the systematic errors are not larger than the statistical errors and the systematics is well understood. This assumption should be reasonable at the time when this application could become relevant.

The most likely case to observe the Earth’s core with supernova neutrinos are baselines crossing the Earth’s outer core, but not the Earth’s inner core, i.e., baselines between about 10;670 km and 12;510 km (about 7% probability for a single detector). Assuming the mantle properties to be known quite well from geophysics, one may then measure the average (outer) core matter density (about 11.4 g/cm^3). As a result of the analysis for the scenario S1 in Tab. 1, it turns out that one could measure this core matter density with a baseline just touching the inner core with about 6% precision with a Super-Kamiokande-

Scenario	ρ_E		ρ_i		Degs
S1	1.0	1.4	2.2	6.4	No
S2	1.0	1.2	5.1	13.6	Yes
S3	0.5	1.4	6.7	16.5	Yes
S4	0.5	1.2	10.2	26.0	Yes

Table 3

The different supernova parameter scenarios from Tab. 1 and the absolute errors ρ_E and ρ_i (in $\text{g}\cdot\text{cm}^{-3}$) for the measurement of ρ_E and ρ_i , respectively, at the 2 σ confidence level with a Super-Kamioke-like detector. In addition, the appearance of degenerate solutions (Degs) at the 2 σ confidence level is indicated.

like detector and 0.9% precision with a Hyper-Kamioke-like detector.

A somewhat more sophisticated application is the combined measurement of the outer and inner core matter densities in the two-parameter model introduced in the last section, i.e., Figs. 4 and 5. In Fig. 6, the results of this analysis are shown in the ρ_E - ρ_i plane for Super-Kamioke- and Hyper-Kamioke-like detectors for the scenario S1 in Tab. 1. One can read off the (absolute) errors at the 2 σ confidence level such as shown in this figure. A Super-Kamioke-like detector cannot verify the inner core, which can be seen in the 2 σ contour crossing the inner core sensitivity line, i.e., the line $\rho_i = 0$. Therefore, it is not well-suited for density measurements of the inner core. However, a Hyper-Kamioke-like detector can clearly observe and verify the inner core even at the 99% confidence level. Furthermore, quite precise measurements of ρ_E and ρ_i are possible. The relative error for ρ_E is about 2.8% and for ρ_i about 50% (2 σ confidence level).

As we have indicated in Sec. 4, the supernova parameter scenarios in Tab. 1 other than the scenario S1 perform somewhat worse in the measurement of the parameters ρ_E and ρ_i . In addition, degenerate solutions appear at the 2 σ confidence level, i.e., different solutions in the parameter space can be fit to the results of the measurement at the considered confidence level. In Tab. 3, we show the errors for the measurement

of ρ_E and ρ_i for the Super-Kamioke detector. It clearly shows that for this application $\rho_E = 1$ and ρ_i large are giving the best results. In addition, degenerate solutions appear for all scenarios except from the scenario S1. It turns out that a somewhat higher ρ_E can improve the results, because it supports the high-energy tail in the spectrum where matter effects are largest.

The results from this measurement cannot be directly compared with the geophysical results, because in seismic wave geophysics the matter density jumps are much easier accessible than the average matter densities. For example, the matter density jump between the outer and inner cores is believed to be about $(0.55 - 0.05) \text{g}\cdot\text{cm}^{-3}$ (see, e.g., Refs. [57(60)]). Translated to the 2 σ confidence level, this corresponds to the same order of magnitude as the Hyper-Kamioke measurement of about 50% precision. However, the average matter density is much harder to access in geophysics and can only be estimated by the long periodic seismic eigenmodes with uncertainties increasing with depth [23]. The precision on the average matter density of about 3% from neutrino physics as well as the measurement of the average matter density jump could help to understand and complement the geophysical information.

Finally, one could consider more than one baseline. If more than one detector observes a supernova through the Earth's core or the inner core, then the potential of this technique would be improved. However, as shown in Tab. 2, the probability for a single detector to have a baseline through the core is already quite low, which means that more detectors would mainly increase the probability that one has an appropriate baseline. Thus, we have in this paper focused on the case of one baseline through the Earth. If really more than one baseline went through the core, then the statistics of the overall measurement would be improved and the result could be estimated by a scaling of the detector. Having one large detector and one baseline corresponds in this application to different detectors at similar positions with their crucial masses adding up to the one of the single detector.

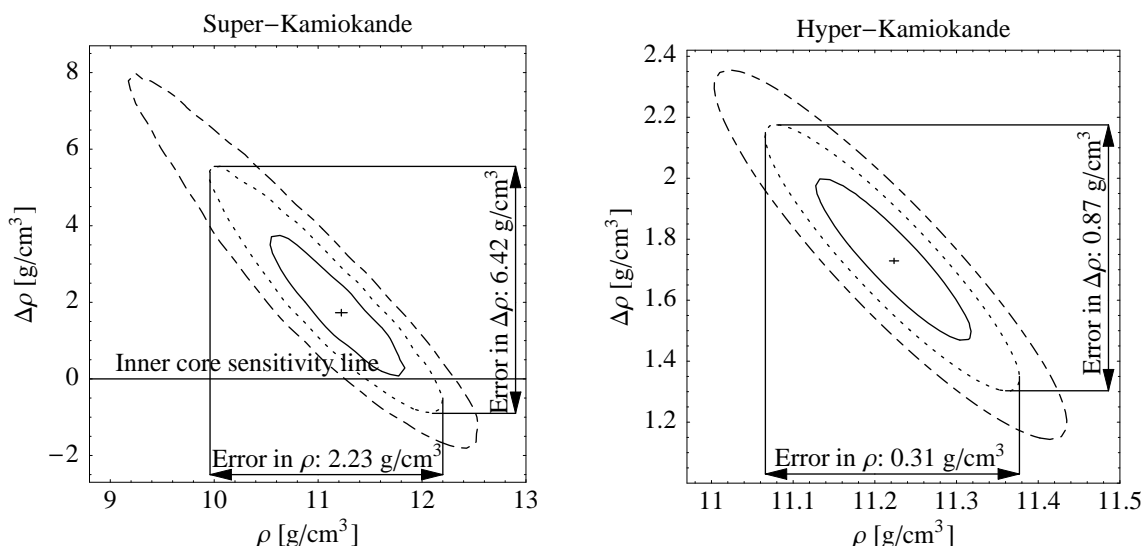


Figure 6. The 1, 2, and 3 contours of the χ^2 -function for a measurement of $\Delta\rho$ and ρ for a Super-Kamiokande-like (left-hand plot) and Hyper-Kamiokande-like (right-hand plot) detector and the scenario S1 in Tab. 1. The errors from statistics and correlations are read off at the arrows in the figures. In order to find evidence for the existence of the inner core (the iron core), the contour of the respective confidence level must not cut the inner core sensitivity line corresponding to $\Delta\rho = 0$. This line can only be seen in the left-hand plot.

7. Uncertainties

In order to discuss the influence of uncertainties on the measurements, we estimate the precision to which the leading neutrino oscillation parameters m_{21}^2 and θ_{12} have to be known for the measurement and we vary them until we observe an effect which is as large as the error of the measurement of $\Delta\rho$ or ρ . It turns out that these leading parameters have to be known with about 1% precision for the Super-Kamiokande-like measurements and with about 0.2% precision for the Hyper-Kamiokande-like measurements. These precisions should be obtainable on the typical timescales of galactic supernova explosions.

The parameter $\sin^2 2\theta_{13}$ also has some influence on the matter effects. For small values, however, the neutrino oscillations reduce to the two-flavor solar case in vacuum. We tested the influence of this parameter on our applications and we found that it can be safely neglected as long as $\sin^2 2\theta_{13}$

is not too large. Only at the CHOOZ bound minor corrections much smaller than the error of our measurements have to be performed. However, this bound will be reduced in the short term future by planned superbeam and neutrino factory experiments (for a summary of expected boundaries see, for example, Ref. [61]).

One of the most important uncertainties in this measurement comes from measuring the electron antineutrinos only. It can be easily seen from Eq. (20) that the extraction of the fluxes of the mass eigenstates from the flux of the electron antineutrino flavor involves assumptions about the supernova parameters, which are entering by the flux ratio f_R . Thus, if only the electron antineutrinos from the supernova can be measured, then the tomography problem will be closely connected to the determination of the supernova parameters at a detector on the surface of the Earth. Estimates for the precision of the supernova parameter determinations are given in Tab. 4, taken

Parameter	SuperK	HyperK	Effects
E_{ν}^{tot}	5%	1% 2%	~ 1%
$E_{\text{e}}^{\text{tot}}$	100%	10%	large
hE_{ν}^{e}	5%	1% 2%	~ 5% 10%
hE_{ν}^{i}	10%	1% 2%	~ 5%

Table 4

The uncertainties on the supernova parameters extracted from the Super-Kamiokande (SuperK) or Hyper-Kamiokande (HyperK) measurements from Ref. [41] and their estimated effects on our parameter measurements as percentage corrections.

from Ref. [41].⁵ In addition, this table shows the estimated influences on the determination of our parameters from a variation of the supernova parameters in the numerical evaluation. The reason for the similar percentage effects for Super-Kamiokande and Hyper-Kamiokande is the parallel scaling of both problems. It is interesting to observe that none of the supernova parameters has a strong influence on the tomography problem except from the overall energy of the muon antineutrinos E_{ν}^{tot} . One can show that this parameter has to be known up to about 20% for the Super-Kamiokande measurement and 3% – 4% for the Hyper-Kamiokande measurement in order not to have strong effects on the tomography problem. However, this precision cannot be achieved by measuring the electron flavor only. Altogether, either E_{ν}^{tot} needs to be measured by different experiments or the fluxes of the muon and tau antineutrinos need to be determined simultaneously with the electron antineutrino flux, making the supernova parameters entirely drop out. This can be seen in Eq. (17), which allows the reconstruction of all mass fluxes at the detector D_1 if all flavor fluxes are measured.

Another issue in the discussion of uncertainties is the parameter Y_e in Eq. (6) relating the number of electrons to the number of nucleons. Since

⁵The results in this reference were obtained for $Y_e = 2.6$, $\mu = 0$, and $\sigma = 0.5$. In this paper, however, we have used slightly different parameter values for which the precisions on the supernova parameters in Tab. 4 would become somewhat worse by about a factor of two.

the Earth matter effects in neutrino oscillations actually depend on the electron density and not on the matter density directly, additional uncertainties enter in the conversion of these two quantities by the parameter Y_e . We assumed $Y_e = 0.5$ in our calculations, but for different materials this parameter can differ somewhat from this value (especially in the inner core. In order to find out the material in each matter density layer, one may prefer to measure the electron density instead of the matter density. However, since in each layer these quantities are proportional to each other, the problem does not change by using the matter density and the electron density can be easily calculated.

8. Summary and conclusions

We have discussed the possibility to use the neutrinos from a future galactic supernova explosion to obtain additional information on the Earth's core. First, we have summarized geophysical aspects and unknowns of the Earth's core. Then, we have investigated core-collapse supernovae as potential neutrino sources for a snapshot of the Earth's interior. Next, we have discussed the neutrino propagation from the production to the detection in detail, where we have especially focused on Earth matter effects on the neutrino oscillations of the supernova neutrinos. We have also put these effects into the context of the supernova parameters, i.e., temperatures and deviation from energy equipartition. Furthermore, we have stressed the importance of supernova neutrinos arriving at the surface of the Earth as mass eigenstates for this technique, which we have also supported by a discussion of decoherence of neutrino oscillations. We have shown that we need one detector on the surface of the Earth on the side towards the supernova, and another one in the shadow of the Earth's core. For the most likely scenario of not crossing the Earth's inner core, we have shown that the Earth's average core matter density could be determined up to 6% with a Super-Kamiokande-like and 0.9% with a Hyper-Kamiokande-like detector (all errors at the 2 σ confidence level). In addition, for a less likely two-parameter measurement of the outer and inner

core matter densities, Hyper-Kamionkande could verify the existence of the inner core at the 3 σ confidence level and measure the outer core matter density with a precision of about 2.8%, as well as the density jump between outer and inner core matter densities with a precision of about 50%. The latter error is comparable to seismic wave geophysics, where, however, not the difference between the average matter densities, but the matter density jump at the outer-inner core boundary is measured. Thus, neutrino physics could provide complementary information to geophysics. Finally, we have discussed several uncertainties to these measurements and we have found that especially the determination of the total muon antineutrino energy of the supernova causes problems to our method. However, measuring not only electron antineutrinos, but also the other two flavors could completely eliminate the dependence on the supernova parameters. Furthermore, the leading solar neutrino parameters have to be known with sufficient precision, which is about 0.2% for Hyper-Kamionkande-like measurements. In summary, supernova neutrino tomography could be a nice additional payoff of existing or planned detectors if all of the prerequisites can be met at the time when the next supernova explodes.

Acknowledgments

We would like to thank Heiner Igel for useful discussions.

This work was supported by the Swedish Foundation for International Cooperation in Research and Higher Education (STINT) [T.O.], the Wenner-Gren Foundations [T.O.], the Swedish Research Council (Vetenskapsrådet), Contract No. 621-2001-1611 [T.O.], the Magnus Bergvall Foundation (Magn. Bergvalls Stiftelse) [T.O.], the "Deutsche Forschungsgemeinschaft" (DFG) [R.T.], the "Studienstiftung des deutschen Volkes" (German National Merit Foundation) [W.W.], and the "Sonderforschungsbereich 375 für Astro-Teilchenphysik der Deutschen Forschungsgemeinschaft" [M.L., T.O., and W.W.].

REFERENCES

1. L.V. Volkova and G.T. Zatsepin, *Bull. Phys. Ser.* 38 (1974) 151.
2. A.D. Rujula et al., *Phys. Rep.* 99 (1983) 341.
3. T.L. Wilson, *Nature* 309 (1984) 38.
4. G.A. Askar'yan, *Usp. Fiz. Nauk* 144 (1984) 523, [*Sov. Phys. Usp.* 27 (1984) 896].
5. A. Borisov, B. Dolgoshein and A. Kalinovski, *Yad. Fiz.* 44 (1986) 681, [*Sov. J. Nucl. Phys.* 44 (1987) 442].
6. A. Nicolaidis, M. Jannane and A. Tarantola, *J. Geophys. Res.* 96 (1991) 21811.
7. H.J. Crawford et al., *Proc. of the XXIVth International Cosmic Ray Conference (University of Rome)* (1995) 804.
8. C. Kuo et al., *Earth Plan. Sci. Lett.* 133 (1995) 95.
9. P. Jain, J.P. Ralston and G.M. Frichter, *Astropart. Phys.* 12 (1999) 193, [hep-ph/9902206](#).
10. V.K. Ermilova, V.A. Tsarev and V.A. Chechin, *Bull. Lebedev Phys. Inst.* NO 3 (1988) 51.
11. V.A. Chechin and V.K. Ermilova, *Proc. of LEW I'90 School, Dubna* (1991) 75.
12. T. Ohlsson and W. Winter, *Phys. Lett. B* 512 (2001) 357, [hep-ph/0105293](#).
13. T. Ohlsson and W. Winter, *Europhys. Lett.* (to be published), [hep-ph/0111247](#).
14. A.N. Ioannisian and A.Y. Smimov, [hep-ph/0201012](#).
15. S.M. Ikhayev and A. Smimov, *Yad. Fiz.* 42 (1985) 1441, [*Sov. J. Nucl. Phys.* 42 (1985) 913].
16. S.M. Ikhayev and A. Smimov, *Nuovo Cim* ento C 9 (1986) 17.
17. L. Wolfenstein, *Phys. Rev. D* 17 (1978) 2369.
18. C. Lunardini and A.Y. Smimov, *Nucl. Phys. B* 616 (2001) 307, [hep-ph/0106149](#).
19. K. Takahashi and K. Sato, [hep-ph/0110105](#).
20. K. Takahashi, M. Watanabe and K. Sato, *Phys. Lett. B* 510 (2001) 189, [hep-ph/0012354](#).
21. K. Aki and P.G. Richards, *Quantitative Seismology - Theory and Methods* (W.H. Freeman, San Francisco, 1980), Vol. 1, 2.
22. T. Lay and T.C. Wallace, *Modern Global*

- Seismology (Academic Press, New York, 1995).
23. H. Igel, private communication.
 24. G. Steinle-Neumann, L. Stixrude and R.E. Cohen, physics/0204055.
 25. G.G. Raelt, Nucl. Phys. Proc. Suppl. 110 (2002) 254, hep-ph/0201099.
 26. H.T. Janka and W. Hillebrandt, Astron. Astrophys. 224 (1989) 49.
 27. H.T. Janka and W. Hillebrandt, Astron. Astrophys. Suppl. 78 (1989) 375.
 28. P.M. Giovanoni, D.C. Ellison and S.W. Bruenn, Astrophys. J. 342 (1989) 416.
 29. H.T. Janka, In *Vulcano 1992, Proceedings, Frontier objects in astrophysics and particle physics* 345-374.
 30. T. Totani et al., Astrophys. J. 496 (1998) 216, astro-ph/9710203.
 31. G.G. Raelt, Astrophys. J. 561 (2001) 890.
 32. R. Buras et al., astro-ph/0205006.
 33. A. Mezzacappa et al., Phys. Rev. Lett. 86 (2001) 1935, astro-ph/0005366.
 34. E.K. Akhmedov, C. Lunardini and A.Y. Smimov, hep-ph/0204091.
 35. A.S. Dighe and A.Y. Smimov, Phys. Rev. D 62 (2000) 033007, hep-ph/9907423.
 36. A.Y. Smimov, D.N. Spergeland J.N. Bahcall, Phys. Rev. D 49 (1994) 1389, hep-ph/9305204.
 37. M. Kachelrie et al., Phys. Rev. D 65 (2002) 073016, hep-ph/0108100.
 38. T. Ohlsson and H. Snellman, Phys. Lett. B 474 (2000) 153, hep-ph/9912295, B 480 (2000) 419 (E).
 39. S.T. Petcov, Phys. Lett. B 434 (1998) 321, hep-ph/9805262, B 444 (1998) 584 (E).
 40. E.K. Akhmedov, Nucl. Phys. B 538 (1999) 25, hep-ph/9805272.
 41. H. Minakata et al., hep-ph/0112160.
 42. C. Giunti, C.W. Kim and U.W. Lee, Phys. Rev. D 44 (1991) 3635.
 43. C. Giunti and C.W. Kim, Phys. Rev. D 58 (1998) 017301, hep-ph/9711363.
 44. W. Grimus, P. Stockinger and S. Mohanty, Phys. Rev. D 59 (1999) 013011, hep-ph/9807442.
 45. C.Y. Cardall, Phys. Rev. D 61 (2000) 073006, hep-ph/9909332.
 46. M. Lindner, T. Ohlsson and W. Winter, Nucl. Phys. B 622 (2002) 429, astro-ph/0105309.
 47. C. Giunti, hep-ph/0205014.
 48. J.N. Bahcall, M.C. Gonzalez-Garcia and C. Pena-Garay, hep-ph/0204314.
 49. CHOOZ Collaboration, M. Apollonio et al., Phys. Lett. B 420 (1998) 397, hep-ex/9711002.
 50. CHOOZ Collaboration, M. Apollonio et al., Phys. Lett. B 466 (1999) 415, hep-ex/9907037.
 51. CHOOZ Collaboration, C. Benford, Nucl. Phys. B (Proc. Suppl.) 77 (1999) 159.
 52. Super-Kamiokande Collaboration, T. Toshito, hep-ex/0105023.
 53. F.D. Stacey, Physics of the Earth, 2 ed. (Wiley, 1977).
 54. A.M. Dziewonski and D.L. Anderson, Phys. Earth Planet. Inter. 25 (1981) 297.
 55. B. Jacobsson et al., Phys. Lett. B 532 (2002) 259, hep-ph/0112138.
 56. Particle Data Group, D.E. Groom et al., Eur. Phys. J. C 15 (2000) 1, <http://pdg.lbl.gov/>.
 57. G. Masters and P. Shearer, J. Geophys. Res. 95 (1990) 21,619.
 58. P. Shearer and G. Masters, Geophys. J. Int. 102 (1990) 491.
 59. M. Ishii and J. Tromp, Science 285 (1999) 1231.
 60. G. Masters, G. Laske and F. Gilbert, Geophys. J. Int. 143 (2000) 478.
 61. P. Huber, M. Lindner and W. Winter, hep-ph/0204352.